Vapor−Liquid Equilibria and Interfacial Tensions of the System Ethanol + 2-Methoxy-2-methylpropane

Andrés Mejía,* Hugo Segura,* and Marcela Cartes

Departamento de Ingeniería Química, Universidad de Concepción, P.O. Box 160C, Correo 3, Concepción 4089100, Chile

Isobaric vapor−liquid equilibrium data have been measured for the binary system ethanol + 2-methoxy-2-methylpropane at (50, 75, and 94) kPa and over the temperature range (308 to 345) K. Equilibrium determinations were performed in a vapor−liquid equilibrium still with circulation of both phases. The dependence of interfacial tensions of this mixture on concentration was also determined at atmospheric pressure and 303.15 K, using the maximum bubble pressure technique. According to experimental results, the mixture exhibits positive deviation from ideal behavior, and azeotropic behavior was observed at (75 and 94) kPa. In addition, the determined interfacial tensions exhibit negative deviation from the linear behavior, and aneotropy is present. The vapor−liquid equilibrium data of the binary mixture satisfy the Fredenlund's consistency test and were well-correlated by the nonrandom two-liquid, Wilson, and UNIQUAC equations for all of the measured isobars. Interfacial tensions, in turn, were satisfactorily correlated using the Redlich−Kister equation.

Introduction

Branched ethers (e.g., 2-methoxy-2-methylpropane or MTBE, 2-ethoxy-2-methylpropane or ETBE, 2-methoxy-2-methylbutane or TAME, or 2,2′-oxybis[propane] or DIPE) are usually combined with alcohols (e.g., methanol, ethanol, or butanol) to synergically improve the octane-enhancing performance of oxygenate additives on fuels. Consequently, vapor−liquid equilibria (VLE) and interfacial tension (IFT) of mixtures composed of alcohols and ethers are of fundamental importance in fuel formulation since, on the one hand, these properties are used to characterize the quality and performance of fuels inside the engine's combustion chamber[1−3] and, on the other hand, the quoted properties play a key role in assessing eventual risks related to the pollution of aquifers during gasoline distribution.[3−5]

Previous works reporting VLE data of ethanol + MTBE cover isobaric determinations at atmospheric pressure[6−8] only, from which it is possible to observe that the mixture exhibits moderate positive deviation from ideal behavior. Azeotropic behavior is also present and persists at temperature above around 309.15 K, as was completely characterized by Gmehling and Bölts,[9] who directly measured the evolution of the azeotrope over the temperature range of (273.15 to 373.15) K. Besides this experimental evidence, Park and Lee[10] reported vapor and liquid phase concentrations at 313.15 K; however, the vapor pressures of the system were not experimentally determined at this isothermal condition, concluding that no azeotrope is present at such a temperature condition.

In contrast to this experimental VLE characterization and to the best of our knowledge, no IFT data have been previously reported for the quoted mixture. Consequently, as part of our ongoing research program on characterizing thermo-physical properties of fuels,[11−15] this contribution is undertaken to report complementary VLE and new IFT data for the ethanol + MTBE mixture, by covering a pressure range over which no data have been previously determined.

* To whom correspondence should be addressed. E-mail: amejia@udec.cl (A.M.) and hsegura@udec.cl (H.S.).

Experimental Section

Purity of Materials. Ethanol was purchased from Merck, and it was used without further purification. MTBE was purchased from Aldrich, and then, it was dried over calcium chloride in a percolation column (50 cm height and 5 cm diameter). The properties and purity of the pure components, as determined by gas chromatography (GC), appear in Table 1.

The densities (ρ) and refractive indexes (n_D) of pure liquids were measured at 298.15 K using an Anton Paar DMA 5000 densimeter (Austria) and a Multiscale Automatic Refractometer RFM 81 (Bellingham and Stanley, England), respectively. During the operation of this equipment, temperature was controlled to within ± 0.01 K by means of a thermostatic bath. The uncertainties in density and refractive index measurements are $5 \cdot 10^{-6}$ g·cm^{-3} and ± 10^{-5}, respectively.

The IFT (σ) of the pure fluids were measured at 303.15 K using a maximum bubble pressure tensiometer, model PC500-LV (Sensadyne, U.S.A.). The uncertainties in IFT measurements are ± 0.1 mN·m^{-1}. Temperature was controlled to within ± 0.1 K with a thermostatic bath (Cole-Palmer, U.S.A.).

The experimental values of physical properties and boiling points of the pure fluids are reported in Table 1 and compared with those given in the literature.

Apparatus and Procedure

Vapor−Liquid Equilibrium Cell. An all-glass VLE apparatus model 601, manufactured by Fischer Labor and Verfahrenstechnik (Germany), was used in the equilibrium determinations. In this circulation-method apparatus, the mixture is heated to its boiling point by a 250 W immersion heater. The vapor−liquid mixture flows through an extended contact line (Cottrell pump) that guarantees an intense phase exchange and then enters to a separation chamber whose construction prevents an entrainment of liquid particles into

10.1021/je9004068 CCC: $40.75
Published on Web 08/11/2009

Table 1. Gas Chromatography (GC) Purities (Mass Fraction), Refractive Index (n_D) at Na D Line, Densities (ρ), Normal Boiling Points (T_b), and IFT (σ) of Pure Components

	n_D		ρ/g·cm^{-3}		T_b/K		σ/mN·m^{-1}	
	T/K = 298.15		T/K = 298.15		P/kPa = 101.33		T/K = 303.15	
component (purity/mass fraction)	exp.	lit.[a]	exp.	lit.[a]	exp.	lit.[a]	exp.	lit.[a]
ethanol (0.999)	1.36068	1.35940	0.78505	0.78589	351.45	351.44	21.70	21.68
MTBE (0.999)	1.36766	1.36630	0.73545	0.73527	328.24	328.35	18.80	18.70

[a] Daubert and Danner.[15]

the vapor phase. The separated gas and liquid phases are condensed and returned to a mixing chamber, where they are stirred by a magnetic stirrer and returned again to the immersion heater. The temperature in the VLE still is determined with a Systemteknik S1224 digital temperature meter and a Pt100 probe calibrated at the Swedish Statens Provningsanstält. The accuracy is estimated as ± 0.02 K. The total pressure of the system is controlled by a vacuum pump capable of work under vacuum up to 0.25 kPa. The pressure is measured with a Fischer pressure transducer calibrated against an absolute mercury-in-glass manometer (22 mm diameter precision tubing with cathetometer reading), and the overall accuracy is estimated as ± 0.03 kPa.

On average the system reaches equilibrium conditions after (2 to 3) h of operation. Samples of 1.0 μL taken by syringe after the system had achieved equilibrium were analyzed by gas chromatography on a Varian 3400 apparatus provided with a thermal conductivity detector and a Thermo Separation Products model SP4400 electronic integrator. The column was 3 m long and 0.3 cm in diameter, packed with SE-30. Column, injector, and detector temperatures were (343.15, 423.15, and 493.15) K, respectively. Good separation was achieved under these conditions, and calibration analyses were carried out to convert the peak area ratio to the mass composition of the sample. The pertinent polynomial fit of the calibration data had a correlation coefficient, R^2, better than 0.99. At least three analyses were made of each sample. The maximum standard deviation of these analyses was 0.08 in area percentage. Concentration measurements were accurate to better than ± 0.001 in mole fraction.

Interfacial Tension Measurements. A maximum bubble pressure tensiometer model PC500-LV manufactured by Sensadyne Inc. (U.S.A.), was used in IFT measurements. In this equipment, two probes of different orifice radii (r_1, r_2) are immersed in a vessel that contains the liquid sample to be measured. Then an inert gas (e.g., nitrogen) is blown through the probes, and the differential pressure (ΔP) between them is recorded. According to the Laplace's equation, ΔP, r_1, and r_2 are related to the IFT, σ, as:

$$\Delta P = P_1 - P_2 = 2\sigma\left(\frac{1}{r_1} - \frac{1}{r_2}\right) \quad (1)$$

where P_i is the pressure exerted by the gas flow in the probe of radius r_i. The gas flow is controlled by a sensor unit connected to a personal computer through an interface board (PCI-DAS08, Measurement Computing, U.S.A.). Besides having a constant volume flow controller, this sensor unit contains a differential pressure transducer, a temperature transducer, and pressure regulator. The temperature of the sample in the vessel is measured by means of a K-type thermocouple and maintained constant to within ± 0.1 K using a thermostatic bath (Cole-Parmer, U.S.A.).

The experimental procedure for determining IFT is as follows. The mixture to be analyzed is prepared by adding appropriate volumes of each pure fluid, and then the concentration of the sample is measured by GC. The sample is then placed into the vessel and heated to the experimental temperature. Thereafter, an inert gas flows through the probes, and the sensor unit translates the voltage signal (Δv) to a ΔP signal. The relation between Δv and ΔP is obtained by calibrating the sensor unit using two reference fluids of well-known IFT (e.g., water and ethanol, respectively). Finally, the IFT is calculated according to eq 1. Additional details concerning the maximum bubble pressure technique have been extensively described by Adamson and Gast[16] and Rusanov and Prokhorov.[17]

Table 2. Experimental VLE Data for Ethanol (1) + MTBE (2) at P = 50.00 kPa[a]

					$-B_{ij}$		
T					cm^3·mol^{-1}		
K	x_1	y_1	γ_1	γ_2	11	22	12
308.30	0.000	0.000		1.000		1908	
308.40	0.046	0.039	3.051	1.004	1848	1906	740
308.58	0.083	0.063	2.720	1.012	1842	1903	739
308.96	0.145	0.094	2.282	1.035	1830	1895	736
309.47	0.213	0.121	1.933	1.072	1813	1885	734
309.94	0.268	0.141	1.747	1.107	1798	1875	731
310.41	0.314	0.154	1.592	1.143	1783	1866	728
310.93	0.368	0.171	1.464	1.194	1767	1856	725
311.26	0.413	0.183	1.371	1.253	1757	1849	724
312.14	0.464	0.205	1.308	1.293	1731	1832	719
312.90	0.515	0.224	1.233	1.359	1708	1818	715
313.62	0.560	0.240	1.171	1.431	1687	1804	711
314.44	0.608	0.262	1.130	1.514	1664	1789	706
315.54	0.655	0.290	1.093	1.597	1633	1769	700
316.99	0.710	0.327	1.057	1.711	1594	1743	693
319.54	0.783	0.398	1.024	1.883	1529	1699	680
321.92	0.834	0.471	1.014	2.000	1471	1659	668
324.74	0.885	0.563	0.996	2.186	1407	1614	655
327.90	0.930	0.682	0.989	2.364	1341	1566	640
330.45	0.960	0.797	0.996	2.485	1290	1529	628
334.57	1.000	1.000	1.000		1215		

[a] T is equilibrium temperature, and x_i and y_i are mole fractions in liquid and vapor phases of component i, respectively. γ_i is the activity coefficient of component i, and B_{ij} is the molar virial coefficient.

Results and Discussion

Vapor−Liquid Equilibrium. The equilibrium temperature, T, liquid-phase of component i, x_i, and vapor-phase of component i, y_i, mole fraction measurements at p = (50, 75, and 94) kPa are reported in Tables 2, 3, and 4 and Figures 1, 2, 3, and 4, together with the activity coefficients (γ_i) that were calculated from the following equation:[18]

$$\ln \gamma_i = \ln \frac{y_i P}{x_i P_i^0} + \frac{(B_{ii} - V_i^L)(P - P_i^0)}{RT} + y_j^2 \frac{\delta_{ij} P}{RT} \quad (2)$$

where P is the total pressure and P_i^0 is the pure component vapor pressure. R is the universal gas constant. V_i^L is the liquid molar volume of component i, B_{ii} and B_{jj} are the second virial

Table 3. Experimental VLE Data for Ethanol (1) + MTBE (2) at P = 75.00 kPa[a]

T					$-B_{ij}$ / cm^3·mol^{-1}		
K	x_1	y_1	γ_1	γ_2	11	22	12
319.39	0.000	0.000		1.000		1702	
319.37	0.046	0.043	2.932	1.004	1533	1702	681
319.47	0.083	0.070	2.609	1.012	1530	1700	680
319.79	0.153	0.109	2.162	1.039	1523	1694	679
320.18	0.216	0.137	1.883	1.073	1513	1688	677
320.66	0.271	0.159	1.700	1.107	1501	1680	674
320.64	0.314	0.174	1.599	1.158	1502	1680	674
320.92	0.368	0.191	1.477	1.220	1495	1676	673
321.40	0.416	0.208	1.393	1.272	1484	1668	671
322.80	0.472	0.231	1.272	1.305	1451	1645	664
323.42	0.517	0.249	1.213	1.366	1437	1635	661
324.14	0.562	0.271	1.169	1.431	1421	1624	657
324.53	0.608	0.291	1.142	1.533	1412	1617	656
326.14	0.659	0.323	1.082	1.600	1377	1592	648
327.54	0.714	0.362	1.048	1.720	1348	1571	642
329.79	0.794	0.443	1.035	1.954	1303	1538	631
332.22	0.838	0.512	1.015	2.024	1257	1504	621
334.68	0.889	0.609	1.017	2.213	1213	1470	610
337.38	0.929	0.708	1.006	2.384	1167	1435	599
339.48	0.957	0.797	1.005	2.568	1133	1408	590
344.02	1.000	1.000	1.000		1064		

[a] T is the equilibrium temperature, and x_i and y_i are mole fractions in liquid and vapor phases of component i, respectively. γ_i is the activity coefficient of component i, and B_{ij} is the molar virial coefficient.

Table 4. Experimental VLE Data for Ethanol (1) + MTBE (2) at P = 94.00 kPa[a]

T					$-B_{ij}$ / cm^3·mol^{-1}		
K	x_1	y_1	γ_1	γ_2	11	22	12
325.98	0.000	0.000		1.000		1596	
325.88	0.045	0.045	2.841	1.004	1383	1596	649
325.92	0.082	0.074	2.581	1.010	1382	1596	649
326.16	0.153	0.117	2.144	1.037	1377	1592	648
326.53	0.216	0.147	1.875	1.070	1369	1587	646
326.86	0.272	0.171	1.695	1.109	1362	1582	645
327.15	0.318	0.190	1.582	1.148	1356	1577	643
327.25	0.368	0.207	1.480	1.210	1354	1576	643
328.29	0.416	0.225	1.356	1.239	1333	1560	638
328.70	0.471	0.245	1.281	1.316	1324	1554	636
329.42	0.516	0.263	1.212	1.373	1310	1544	633
329.90	0.561	0.286	1.186	1.446	1301	1537	631
331.27	0.608	0.315	1.129	1.492	1274	1517	625
332.32	0.659	0.343	1.082	1.595	1255	1502	620
333.75	0.715	0.386	1.052	1.708	1229	1483	614
336.14	0.797	0.473	1.037	1.922	1187	1451	604
338.76	0.847	0.542	0.998	2.060	1144	1417	593
340.65	0.891	0.628	1.013	2.230	1115	1394	586
343.32	0.928	0.721	0.998	2.374	1075	1361	575
345.39	0.957	0.810	0.998	2.569	1045	1337	567
349.56	1.000	1.000	1.000		989		

[a] T is the equilibrium temperature, and x_i and y_i are mole fractions in liquid and vapor phases of component i, respectively. γ_i is the activity coefficient of component i, and B_{ij} is the molar virial coefficient.

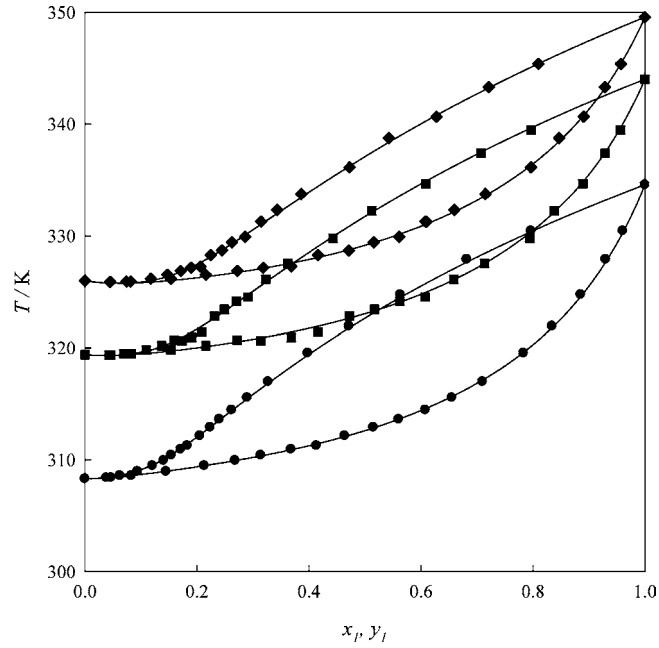

Figure 1. Boiling temperature (T) as a function of the liquid mole fraction (x_1) for the system ethanol (1) + MTBE (2). Experimental data: ●, 50.00 kPa; ■, 75.00 kPa; ◆, 94.00 kPa; solid line, smoothed by fitting a threeparameter Legendre polynomial.

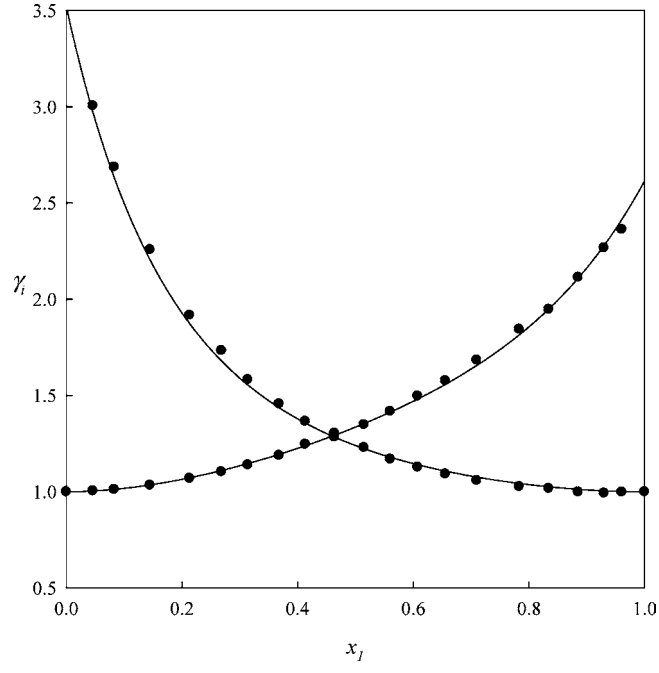

Figure 2. Activity coefficients (γ_i) as a function of the liquid mole fraction (x_1) for the system ethanol (1) + MTBE (2) at 50.00 kPa. ●, experimental data; solid line, smoothed by fitting a three-parameter Legendre polynomial.

coefficients of the pure gases, and B_{ij} is the cross second virial coefficient. The mixing rule of second virial coefficients (δ_{ij}) is given by

$$\delta_{ij} = 2B_{ij} - B_{jj} - B_{ii} \quad (3)$$

According to eq 2, the standard state for calculating activity coefficients is the pure component at the pressure and temperature of the solution. Equation 2 is valid from low to moderate pressures, where the virial equation of state truncated after the second term is adequate for describing the vapor phase of the pure components and their mixtures, and additionally, the liquid molar volumes of pure components are incompressible over the pressure range under consideration. Liquid molar volumes were estimated from the correlation proposed by Rackett.[19] Critical properties were taken from Daubert and Danner.[15] The molar virial coefficients B_{ii}, B_{jj}, and B_{ij} were estimated by the method of Hayden and O'Connell[20] using the molecular and solvation parameters η suggested by Prausnitz et al.[21] for the case of ethanol. For the case of MTBE, molecular parameters and physical properties were also taken from ref 15, while the solvation parameter was estimated by smoothing experimental

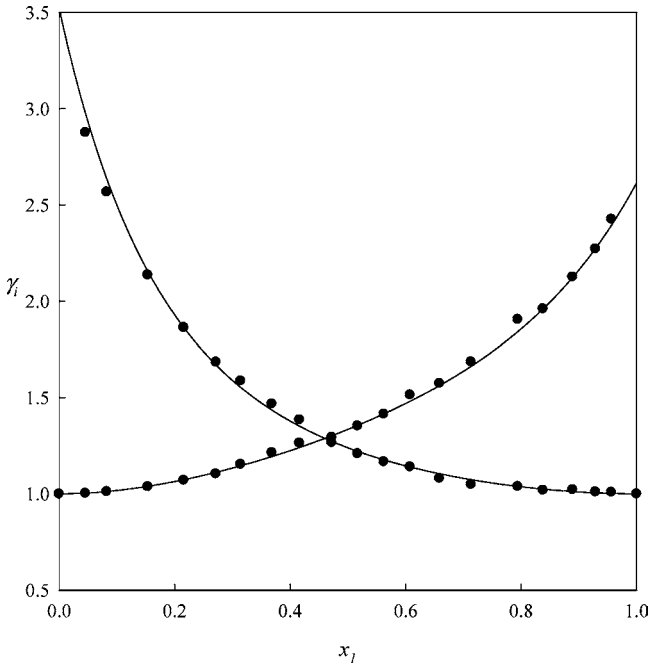

Figure 3. Activity coefficients (γ_i) as a function of the liquid mole fraction (x_1) for the system ethanol (1) + MTBE (2) at 75.00 kPa. ●, experimental data; solid line, smoothed by fitting a three-parameter Legendre polynomial.

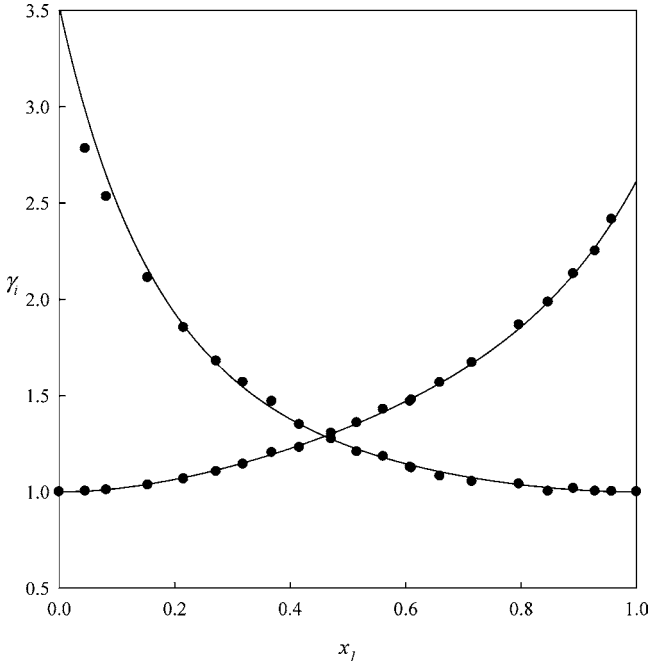

Figure 4. Activity coefficients (γ_i) as a function of the liquid mole fraction (x_1) for the system ethanol (1) + MTBE (2) at 94.00 kPa. ●, experimental data; solid line, smoothed by fitting a three-parameter Legendre polynomial.

data of second virial coefficients reported in ref 15, thus yielding the value $\eta = 0.078$. B_{ii}, B_{jj}, and B_{ij} values are reported in Tables 2 to 4.

The vapor pressure of the pure components was experimentally determined as a function of temperature using the same equipment as that for obtaining the VLE data. The experimental values for MTBE have been previously reported elsewhere,[14] while Table 5 presents the experimental values obtained for ethanol. The temperature dependence of the vapor pressure P_i^0 was correlated using the Antoine equation:

$$\log(P_i^0/\text{kPa}) = A_i - \frac{B_i}{(T/\text{K}) + C_i} \quad (4)$$

where the Antoine constants A_i, B_i, and C_i are reported in Table 6. Equation 4 correlated the vapor pressure data of ethanol with an average of the absolute percentage deviation (AAPD) of 0.10 %. Figure 5 shows a comparison between the vapor pressure predicted from eq 4 with the parameters presented in Table 6 and the experimental data reported by Ambrose et al.[22] From this figure it is possible to conclude about the reliability of the parameters presented in Table 6, since they predict very well the values reported by Ambrose et al., with an AAPD of 0.07 %.

The activity coefficients presented in Tables 2 and 4 are estimated accurate to within ± 1.5 %. The experimental data reported in these tables allow the conclusion that the binary mixtures exhibit positive deviation from ideal behavior, and

Table 5. Experimental Vapor Pressures (*P*) as a Function of Temperature (*T*) for Ethanol

T / K	*P* / kPa
310.89	16.01
318.88	24.01
323.51	30.01
328.54	38.01
332.24	45.01
335.05	51.01
338.38	59.01
341.01	66.01
343.40	73.01
345.61	80.01
347.66	87.01
349.58	94.01
351.65	102.07

Table 6. Antoine Coefficients (A_i, B_i, and C_i) in Equation 4

compound	A_i	B_i	C_i	temperature range/K
ethanol	7.16178	1549.6973	−50.890	310.89 to 351.65
MTBE[a]	6.12370	1184.1727	−40.674	301.31 to 328.24

[a] Parameters have been taken from ref 14.

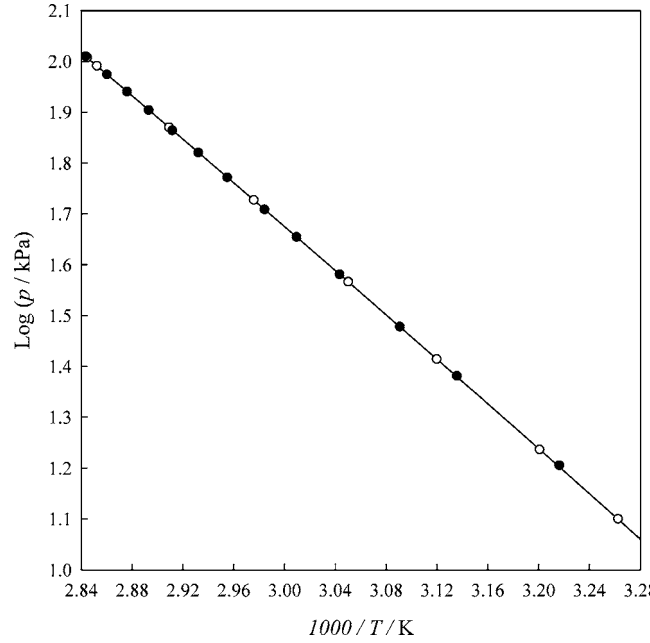

Figure 5. Vapor pressure (*P*) as a function of temperature (*T*) for ethanol. Solid line, predicted by eq 4 and parameters reported in Table 6. Experimental data: ●, this work; ○, Ambrose and Sprake.[22]

Table 7. Estimated Azeotropic Coordinates for the System Ethanol (1) + MTBE (2)[a]

P / kPa	x_1^{Az}	T^{Az} / K
50		
75	0.037	319.32
94	0.062	325.77

[a] P is the pressure of the system, x_1^{Az} the azeotropic mole fraction, and T^{Az} the azeotropic temperature.

Table 8. Consistency Test Statistics for the Binary System Ethanol (1) + MTBE (2)

P / kPa	L_1[a]	L_2[a]	L_3[a]	$100\cdot\Delta y$[b]	δP[c] / kPa
50.00	1.0643	−0.1536	0.0492	0.3	0.1
75.00	1.1022	−0.1466	0.0815	0.3	0.6
94.00	1.0769	−0.1451	0.0702	0.4	0.5

[a] Parameters for the Legendre polynomial[24] used in consistency. [b] Average absolute deviation in vapor phase mole fraction: $\Delta y = (1/N)\sum_{i=1}^{N}|y_i^{exp} - y_i^{cal}|$ (N: number of data points). [c] Average absolute deviation in vapor pressure: $\delta P = (1/N)\sum_{i=1}^{N}|P_i^{exp} - P_i^{cal}|$.

azeotropy is confirmed at (75 and 94) kPa. However, no azeotrope has been detected at 50 kPa. The azeotropic concentrations of the measured binaries were estimated by fitting the function

$$f(x) = 100\left(\frac{y - x}{x}\right) \qquad (5)$$

where $f(x)$ is an empirical interpolating function and x and y have been taken from the experimental data. Azeotropic concentrations, as determined by solving $f(x) = 0$, are indicated in Table 7. These azeotropic coordinates are in good agreement to results presented by Gmehling and Bölts.[9]

The VLE data reported in Tables 2 to 4 were found to be thermodynamically consistent by the point-to-point method of Van Ness et al.[23] as modified by Fredenslund et al.[24] For each isobaric condition, consistency criterion ($\Delta y < 0.01$) was met by fitting the equilibrium vapor pressure according to the Barker's[25] reduction method. Statistical analysis reveals that a three-parameter Legendre polynomial is adequate for fitting the equilibrium vapor pressure in each case. Pertinent consistency statistics and Legendre polynomial parameters are presented in Table 8.

The VLE data reported in Tables 2 to 4 were correlated with the Wohl, nonrandom two-liquid (NRTL), Wilson, and UNIQUAC equations,[26] whose adjustable parameters were obtained by minimizing the following objective function (OF):

$$\mathrm{OF} = \sum_{i=1}^{N}(|P_i^{exp} - P_i^{cal}|/P_i^{exp} + |y_i^{exp} - y_i^{cal}|)^2 \qquad (6)$$

In eq 6, the superscript exp represents experimental data while cal means calculate quantity. N is the number of data points. Pertinent parameters are reported in Table 9, together with the relative deviation for the case of bubble and dew point pressures. From the results presented in Table 9, it is possible to conclude that all the fitted models gave a reasonable correlation of the binary system; the best fit is obtained with the Wilson model. The capability of predicting simultaneously the bubble- and dew-point pressures and the vapor and liquid phase mole fractions, respectively, has been used as the ranking factor. To establish the coherency of the present binary data and to test the predictive capability of the parameters reported in Table 9, we have used the best ranked model (Wilson's model) to predict the binary

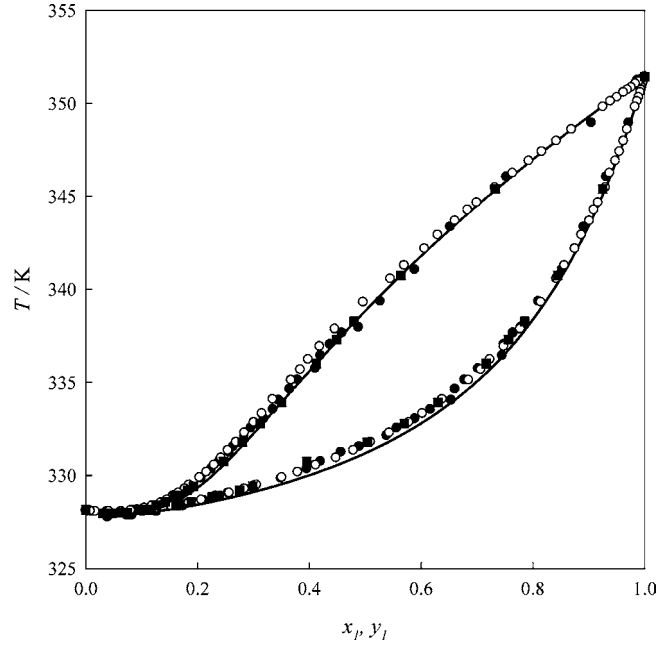

Figure 6. Boiling temperature (T) as a function of the liquid mole fraction (x_1) for the system ethanol (1) + MTBE (2) at 101.3 kPa. Solid line, predicted from the Wilson model with the parameters indicated in Table 9. Experimental data reported by: ○, Arce et al.;[6] ■, Hiaki et al.;[7] ●, Park et al.[8]

Table 9. Parameters and Prediction Statistics for Different Gibbs Excess (G^E) Models in Ethanol (1) + MTBE (2)[a]

model	P / kPa	A_{12}	A_{21}	α_{12}	bubble-point pressures ΔP (%)[b]	bubble-point pressures $100\cdot\Delta y_i$[c]	dew-point pressures ΔP (%)[b]	dew-point pressures $100\cdot\Delta x_i$[c]
Wohl	50.00	1.225	0.927	1.308[d]	0.42	0.2	0.58	0.3
	75.00	1.244	0.944	1.319[d]	0.93	0.3	0.85	0.5
	94.00	1.244	0.944	1.319[d]	0.86	0.3	0.88	0.5
NRTL	50.00	553.43	2664.69	0.300[e]	0.50	0.3	0.76	0.5
	75.00	556.77	2831.31	0.300[e]	1.00	0.4	0.95	0.7
	94.00	725.43	2611.99	0.300[e]	0.65	0.5	0.82	0.9
Wilson[f]	50.00	4591.57	−1188.95		0.17	0.3	0.50	0.4
	75.00	4848.67	−1207.13		0.95	0.3	0.93	0.5
	94.00	4730.79	−1138.54		0.64	0.4	0.81	0.6
UNIQUAC[g]	50.00	−801.56	2167.40		0.37	0.3	0.60	0.4
	75.00	−849.66	2310.59		0.98	0.3	0.92	0.6
	94.00	−794.77	2203.63		0.63	0.4	0.77	0.7

[a] A_{12} and A_{21} are the G^E model parameters in J·mol^{-1}. [b] $\Delta P = (100/N)\sum_i^N|P_i^{exp} - P_i^{cal}|/P_i^{exp}$. [c] $\Delta\delta = 1/N\sum_i^N|\delta_i^{exp} - \delta_i^{cal}|$ with $\delta = y$ or x. [d] "q" parameter for the Wohl's model. [e] "α_{12}" parameter for the NRTL's model. [f] Liquid molar volumes have been estimated from the Rackett equation.[19] [g] Molecular parameters are those calculated from UNIFAC[24,27] using the following r and q parameters: $r_1 = 2.5755$, $r_2 = 4.0678$, $q_1 = 2.588$, and $q_2 = 3.632$.

Table 10. IFT (σ) as a Function of the Liquid Mole Fraction (x_1) for the Binary System Ethanol (1) + MTBE (2) at 303.15 K and 101.3 kPa

x_1	σ / mN·m^{-1}
0.000	18.80
0.102	18.39
0.212	18.38
0.310	18.54
0.408	18.84
0.527	19.00
0.623	19.21
0.721	19.56
0.826	20.03
0.921	20.57
1.000	21.70

VLE data reported in other sources. Results are shown in Figure 6, where we can observe a very good agreement both in the predicted bubble-point ($\Delta P = 1.0$ %, $\Delta y_i = 0.56$ %) and dew-point pressures ($\Delta P = 0.93$ %, $\Delta x_i = 0.77$ %).

Interfacial Tension Data. The IFT measurements at $T = 303.15$ K and $P = 101.3$ kPa are reported in Table 10 and depicted in Figure 7. These experimental data were correlated using the following Redlich−Kister expansion[28]

$$\sigma = x_1 x_2 \sum_{k=0}^{m} c_k (x_1 - x_2)^k + x_1\sigma_1 + x_2\sigma_2 \qquad (7)$$

In eq 7, σ is the IFT of the mixture, while σ_i is the IFT of the pure components. m denotes the number of c_k parameters.

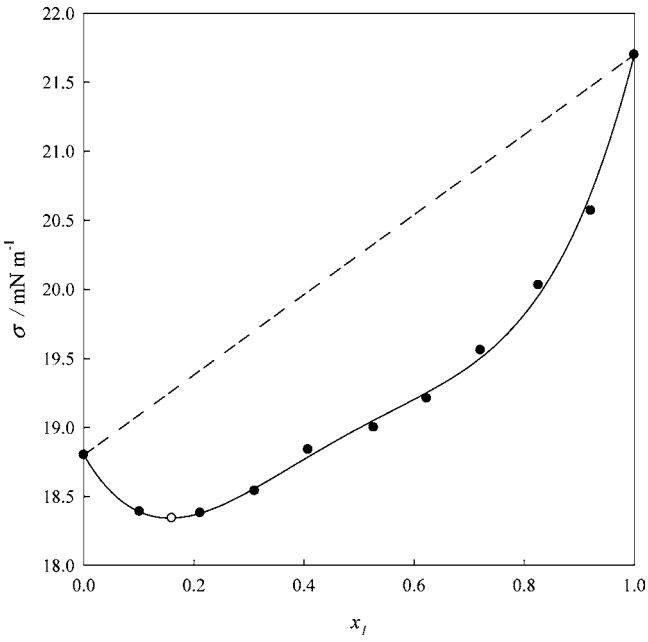

Figure 7. IFT (σ) as a function of the liquid mole fraction (x_1) for the system ethanol (1) + MTBE (2) at 303.15 K and 101.3 kPa. ●, experimental data; solid line, smoothed by a Redlich−Kister expansion with the parameters shown in Table 11; dashed line, linear behavior; ○, aneotropic point.

Table 11. Coefficients (c_0, c_1, and c_2) and Deviations (Maximum (max dev), Average (avg dev), and Standard (st dev)) Obtained in the Correlation of IFT, Eq 7, for the Ethanol (1) + MTBE (2) at 303.15 K and 101.3 kPa

mN·m^{-1}			10^3·mN·m^{-1}		
c_0	c_1	c_2	max dev	avg dev	st dev
−5.0183	1.5114	−6.2050	15.68	2.94	4.41

The c_k parameters of eq 7 were obtained by a Simplex optimization technique, and pertinent results together with the correlation statistics are reported in Table 11. From Figure 7 it is possible to conclude that the IFT of the mixture ethanol + MTBE exhibits negative deviation from the linear behavior ($x_1\sigma_1 + x_2\sigma_2$), and aneotropy is present at $x_1 \approx 0.16$.

Conclusions

Isobaric VLE data at (50, 75, and 94) kPa and atmospheric IFT at 303.15 K have been reported for ethanol + MTBE. Experimental results revealed that the phase equilibrium data for this binary mixture exhibits positive deviations from ideal behavior, and azeotropic behavior is present at (75 and 94) kPa. The IFT of the analyzed mixture exhibits negative deviation from linear behavior, and aneotropic behavior is present at $x_1 \approx 0.16$.

The activity coefficients and boiling points of ethanol + MTBE were well-correlated with the mole fraction using the NRTL, Wilson, and UNIQUAC equations, the best fit corresponding to the Wilson model. The IFT of this mixture were smoothed using the Redlich−Kister equation.

Literature Cited

(1) Weber de Menezes, E.; Cataluna, R.; Samios, D.; da Silva, R. Addition of an azeotropic ETBE/ethanol mixture in eurosuper-type gasolines. *Fuel* **2006**, *85*, 2567–2577.
(2) Józwiak, D.; Szlek, A. Ignition characteristics of vegetable fuel oils in fuel spray. *J. Energy Inst.* **2007**, *80*, 35−39.
(3) French, R.; Malone, P. Phase equilibria of ethanol fuel blends. *Fluid Phase Equilib.* **2005**, *228–229*, 27–40.
(4) de Pereira, P. A.; Santos, L. M. B.; Sousa, E. T.; de Andrade, J. B. Alcohol- and Gasohol-Fuels: A comparative chamber study of photochemical ozone formation. *J. Braz. Chem. Soc.* **2004**, *15*, 646–651.
(5) Ahmed, F. E. Toxicology and human health effects following exposure to oxygenated or reformulated gasoline. *Toxicol. Lett.* **2001**, *123*, 89–113.
(6) Arce, A.; Martinez-Ageitos, J.; Soto, A. VLE measurements of binary mixtures of methanol, ethanol, 2-methoxy-2-methylpropane, and 2-methoxy-2-methylbutane at 101.32 kPa. *J. Chem. Eng. Data* **1996**, *41*, 718–723.
(7) Hiaki, T.; Tatsuhana, K.; Tsuji, T.; Hongo, M. Isobaric vapor-liquid equilibria for 2-methoxy-2-methylpropane + ethanol + octane and constituent binary systems at 101.3 kPa. *J. Chem. Eng. Data* **1999**, *44*, 323–327.
(8) Park, S. J.; Han, K. J.; Gmehling, J. Vapor-liquid equilibria and excess properties for methyl tert-butyl ether (MTBE) containing binary systems. *Fluid Phase Equilib.* **2002**, *200*, 399–409.
(9) Gmehling, J.; Bölts, R. Azeotropic data for binary and ternary systems at moderate pressures. *J. Chem. Eng. Data* **1996**, *41*, 202–209.
(10) Park, S. J.; Lee, T. J. Vapor-liquid equilibria and excess molar properties of MTBE + methanol and ethanol mixtures. *Korean J. Chem. Eng.* **1995**, *12*, 110–114.
(11) Mejía, A.; Segura, H.; Cartes, M.; Bustos, P. Vapor - liquid equilibrium, densities, and interfacial tensions for the system ethyl 1,1-dimethylethyl ether (ETBE) + propan-1-ol. *Fluid Phase Equilib.* **2007**, *255*, 121–130.
(12) Mejía, A.; Segura, H.; Cartes, M. Vapor - liquid equilibrium, densities, and interfacial tensions for the system benzene + propan-1-ol. *Phys. Chem. Liq.* **2008**, *46*, 185–200.
(13) Mejía, A.; Segura, H.; Cartes, M.; Calvo, C. Vapor - liquid equilibria and interfacial tensions for the ternary system acetone + 2,2′-oxybis[propane] + cyclohexane and its constituent binary systems. *Fluid Phase Equilib.* **2008**, *270*, 75–86.
(14) Mejía, A.; Segura, H.; Cartes, M.; Cifuentes, L.; Flores, M. Phase equilibria and interfacial tensions in the systems methyl tert-butyl ether + acetone + cyclohexane, methyl tert-butyl ether + acetone and methyl tert-butyl ether + cyclohexane. *Fluid Phase Equilib.* **2008**, *273*, 68–77.
(15) Daubert, T. E.; Danner, R. P. *Physical and Thermodynamic Properties of Pure Chemicals. Data Compilation*; Taylor and Francis: Bristol, PA, 1989.
(16) Adamson, A. W.; Gast, A. P. *Physical Chemistry of Surfaces*: Wiley Interscience: New York, 1997.

(17) Rusanov, A. I.; Prokhorov, V. A. *Interfacial Tensiometry*, Elsevier: Amsterdam, 1996.
(18) Van Ness, H. C.; Abbott, M. M. *Classical Thermodynamics of Nonelectrolyte Solutions*, McGraw-Hill Book Co.: New York, 1982.
(19) Rackett, H. G. Equation of state for saturated liquids. *J. Chem. Eng. Data* **1970**, *15*, 514–517.
(20) Hayden, J.; O'Connell, J. A generalized method for predicting second virial coefficients. *Ind. Eng. Chem. Process Des. Dev.* **1975**, *14*, 209–216.
(21) Prausnitz, J. M.; Anderson, T.; Grens, E.; Eckert, C.; Hsieh, R.; O'Connell, J. *Computer Calculations for Multicomponent Vapor - Liquid and Liquid - Liquid Equilibria*, Prentice - Hall: New York, 1980.
(22) Ambrose, D.; Sprake, C. H. S. Vapor Pressure of Alcohols. *J. Chem. Thermo.* **1970**, *2*, 631–645.
(23) Van Ness, H. C.; Byer, S. M.; Gibbs, R. E. Vapor - liquid equilibrium: Part I. An appraisal of data reduction methods. *AlChE J* **1973**, *19*, 238–244.
(24) Fredenslund, Aa.; Gmehling, J.; Rasmussen, P. *Vapor-Liquid Equilibria Using UNIFAC, A Group Contribution Method*. Elsevier: Amsterdam, 1977.
(25) Barker, J. A. Determination of Activity Coefficients from total pressure measurements. *Aust. J. Chem.* **1953**, *6*, 207–210.
(26) Prausnitz, J. M.; Lichtenthaler, R. N.; Gomes de Azevedo, E. *Molecular Thermodynamics of Fluid-Phase Equilibria*, 3th ed., Prentice-Hall: NJ, 1999.
(27) Wittig, R.; Lohmann, J.; Gmehling, J. Vapor-Liquid Equilibria by UNIFAC Group Contribution. 6. Revision and Extension. *Ind. Eng. Chem. Res.* **2003**, *42*, 183–188.
(28) Myers, D. B.; Scott, R. L. Thermodynamic functions for nonelectrolyte solutions. *Ind. Eng. Chem* **1963**, *55*, 43–46.

Received for review May 7, 2009. Accepted July 29, 2009. This work was financed by FONDECYT, Santiago, Chile (Project 1080596).

JE9004068